Transient characteristics and optimal control strategy of superconducting controllable reactor

Características transitorias y estrategia óptima de control de un reactor controlable superconductor

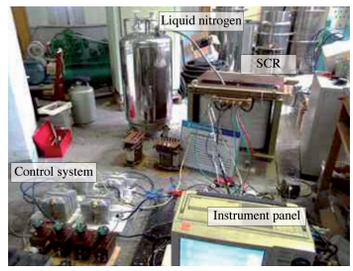

Bo Chen[1], Na Yu[1,*], Xuanyao Luo[2], Lei Liu[2], Xiang Li[2,5], Bin Sun[3], and Zhangting Yu[4]

[1] School of Information Science and Engineering, Wuhan University of Science and Technology, 947 Peace Avenue, Qingshan District, Wuhan 430081, Hubei, China. Correspongding author: Na Yu, email: m13517129418_1@163.com
[2] School of Electrical Engineering, Wuhan University, 299 Bayi Street, Wuchang District, Wuhan 430072, Hubei, China
[3] Institue of Economy and Technology of Huanggang Power Supply Company, 36 Dongmen Street, Huangzhou District, Huanggang 438000, Hubei, China
[4] Guangxi Grid Company, LTD Electirc Power Research Institute, 6-2, Minzhu Street, Nanning 530000, Guangxi, China
[5] Department of Electrical and Electronic Engineering Saga University, 1 Honjo-machi, Saga, 840-8502, Japan

DOI: http://dx.doi.org/10.6036/8186 | Recibido: 26/09/2016 • Aceptado: 29/11/2016

RESUMEN

• El Reactor Controlable Superconductor (SCR) es un equipo prometedor para compensar la potencia reactiva y mejorar la estabilidad de la tensión y la fiabilidad de un sistema energético. Dada la especial estructura y la complejidad del circuito magnético del SCR, falta un análisis en profundidad de las características transitorias y de la estrategia de control que tienen un importante efecto sobre su rendimiento. En este estudio se propone un análisis de las características transitorias y una estrategia óptima de control. En primer lugar, se presenta el principio básico de la operación y la impedancia del modelo analítico del SCR. Después, se analizan detalladamente las características transitorias en el componente de corriente continua (DC) y la sobretensión, proponiéndose una estrategia óptima de control basada en un interruptor de circuito y en tiristores anti-paralelos. Finalmente se validan el principio y los resultados de los métodos propuestos por simulación electromagnética y por experimentos con un prototipo a 380V/30kVar. Los resultados de la simulación y los experimentos demuestran que el componente de DC y la sobretensión se producen en el proceso transitorio. Cuando el ángulo de conexión del arrollamiento superconductor es de 90º, el componente de DC y la sobretensión son pequeños. El sistema de control óptimo propuesto puede evitar la producción del componente de DC y sobretensión que dañarían los arrollamientos superconductores. Los resultados obtenidos por este estudio podrán ser aplicados en el diseño de SCR con rendimientos óptimos.

• **Palabras clave:** Reactor Controlable Superconductor, Estrategia de control óptimo, Componente de DC, Sobretensión.

ABSTRACT

Superconducting controllable reactor (SCR) is a promising device for reactive power compensation to improve the voltage stability and reliability of power system. Given the special structure and complex magnetic circuit of SCR, the transient characteristics and control strategy, which have an important effect on the performance of SCR, lack comprehensive analysis. In this study, transient characteristics analysis and an optimal control strategy are proposed. First, the basic operating principle and the impedance of the analytical model of SCR were presented. Second, the transient characteristics on the DC component and the overvoltage of SCR were analyzed in detail, and an optimal control strategy based on circuit breaker and anti-parallel thyristors was proposed. Finally, the principle and performance of proposed methods were validated through electromagnetic simulation and experiments of 380V/30kVar prototype. The simulation and experimental results demonstrate that the DC component and overvoltage will be produced in the transient process. When the switching angle of superconducting winding is 90°, the DC component and overvoltage become small. The optimal control system proposed can avoid producing the DC component and overvoltage that damage the superconducting windings. The results obtained in this study can be applied to the optimal performance design of SCR.

Keywords: Superconducting controllable reactor, Optimal control strategy, DC component, Overvoltage.

1. INTRODUCTION

With the widely use of high-power fluctuating loads and the continuous growth of distributed sustainable energies, reactive power fluctuation of high-voltage power system has been becoming a serious problem, which will reduce the power quality, power factor and lead to voltage fluctuation [1]. To solve these issues, reactive power compensation devices should be installed in the high-voltage power system [2-4]. Traditional reactive power compensation measures mainly include installing the synchronous compensator and fixed capacitor. The synchronous compensator is one of the earliest devices for reactive power compensation. This device is similar to a synchronous motor under no-load conditions. The synchronous compensator can provide dynamic reactive power compensation by adjusting the exciting current. However, given the disadvantages of large loss, high noise, and complex maintenance, the use of synchronous compensator is limited to the high-voltage power system. In addition, fixed capacitor is one of the most commonly used devices for reactive power compensation in the power system. This device is low cost, easy to install, and low maintenance. Considering that fixed capacitor can provide the fixed capacitive reactive power, the harmonic currents of power system may be amplified by the fixed capacitor, and the response speed is so slow that it cannot satisfy the dynamic reactive power compensation requirements of high-voltage power system. Hence, studying effective reactive power compensation devices in high-voltage power grid is necessary.

2. STATE OF THE ART

At present, reactive power compensation devices, which have been attracting worldwide attention from researchers and companies, mainly include thyristor controlled reactor (TCR), saturable reactor (SR), and static var generation (SVG) [5-12]. A thyristor-controlled reactor was used for power factor correction and terminal voltage stabilization of power system in [5]. A combined system of a TCR and a shunt hybrid power filter was proposed to provide the harmonic and reactive power compensation in [6]. TCR can adjust the reactive power by changing the trigger angle of thyristors. However, the withstanding voltage and harmonics of TCR limit its development. A saturable two-stage magnetic controlled reactor was proposed for arc suppression in [7-8]. A saturable continuously variable series reactor was presented to power flow control in [9]. However, the saturable reactor (SR) is limited by its harmonics and response speed. In addition, SVG can flexibly compensate the reactive power of power system and has low harmonics via control strategy. Static synchronous compensators, as a type of SVG, was presented to provide unbalanced voltage support in unbalanced power systems [10-11]. A cascaded static var generator (SVG) with delta-configuration was discussed for a compensation of reactive, negative-sequence, and harmonic currents in [12]. A single-phase full-bridge configuration of static var generators (SVG) was used with reduced equipped capacitance for reactive power compensation in [13]. However, considering that the power electronic devices can only withstand low voltage, SVG is difficult to apply in high-voltage power grids.

With the development of second-generation high-temperature superconducting technology, superconducting controllable reactor (SCR) has been one of the most promising reactive power compensation devices in the power system. Its advantages are its free harmonics, fast response speed, low losses, and ability to withstand high voltage [14–16]. The leakage inductance and reactive capacity of SCR can be adjusted by shortening the superconducting windings. Researchers have analyzed the principle and steady-state performance of SCR [16]. However, the transient characteristics and control strategy of SCR require additional attention.

The output capacity of SCR is adjusted by switching on/off the superconducting windings. When the superconducting windings are switched on/off at the different angles of system voltage, the DC component and overvoltage will be produced in the superconducting windings. The DC component may produce more losses and lead to superconducting quench. The overvoltage will cause the insulation damage of the superconducting windings. Therefore, the control strategy of SCR should be optimized to avoid producing DC component and overvoltage, and the optimal control strategy of SCR should be a greater focus. SCR should be designed to have several gears to adjust the output capacity, thereby meeting the requirements of reactive power compensation. The key problem of capacity gear design of SCR is impedance calculation. Hence, based on the basic principle and mathematical impedance model, this paper analyzes the transient characteristics of SCR via the theory and finite element analysis method (FEA) [17]; the DC component and overvoltage produced in transient process will have an important effect on the performance. Finally, this paper presents an optimal control strategy to effectively avoid the DC component and overvoltage.

The remainder of this paper is organized as follows: Section 3 describes the operating principle, the transient characteristics, and the optimal control strategy of SCR. Then, Section 4 presents various simulations via FEA method to analyze the transient characteristics of SCR, and presents a real 380V/30kVar experiment to evaluate the performance and transient control characteristics of SCR with optimal control system. Lastly, Section 5 concludes.

3. METHODOLOGY

3.1. OPERATING PRINCIPLE OF SCR

Fig.1 shows the structure of SCR, which consists of the windings, cores, controlling system, and cooling system. SCR includes a working winding and two superconducting windings. The working winding is connected to electrical power system to supply reactive power compensation, whereas two superconducting windings are used as the controlled windings to adjust the output capacity of SCR. The controlling system can control the on/off conditions of superconducting windings B and C. The flux path can be changed by the on/off conditions of superconducting windings. Hence, the reactance of SCR can be adjusted.

Considering that the structure of this device is similar to that of a transformer, the equivalent circuit of SCR is shown in Fig.2. The on/off conditions of superconducting windings can be represented by switches K_1 and K_2. X_A, X_B, and X_C represent the equivalent reactance of working winding A and two superconducting windings B and C, respectively. Based on on/off states of superconducting windings, SCR has four working modes and four capacity gears, as shown in Table I.

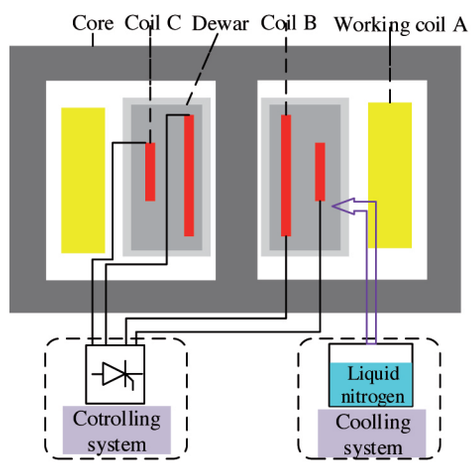

Fig. 1: Structural topology of SCR

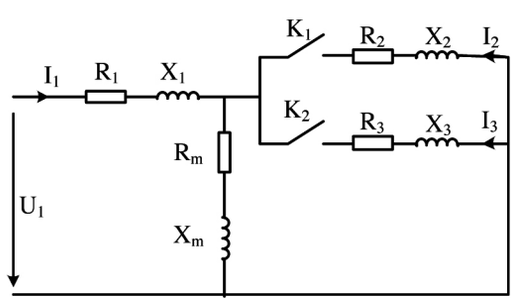

Fig. 2: Circuit principle of SCR

Capacity gear	Superconducting winding B (K_1)	Superconducting winding C (K_2)	Reactance
G1	off	off	X_{G1}
G2	off	on	X_{G2}
G3	on	off	X_{G3}
G4	on	on	X_{G4}

Table I:. Working gear of SCR

For a winding with n layers [18–19], the magnetic conductance matrix of this winding is

$$P=\begin{bmatrix} P_{11} & & P_{1n} \\ & \ddots & \\ P_{n1} & & P_{nn} \end{bmatrix} \tag{1}$$

$$P_{ij}=\frac{\lambda_i}{i_j} \tag{2}$$

where $P_{ij}=P_{ji}$. P matrix can be obtained via FEA simulation for n times. λ_i is the flux linkage of coil i with current i_j.

Hence, the inductance matrix of the winding can be calculated as

$$L_{ij}=N_iN_jP_{ij} \tag{3}$$

where N_i and N_j represent the number of coil turns in layer i and j, respectively.

We assume that three windings of SCR contain n_A, n_B, and n_C layers. $A(i)$, $B(i)$, and $C(i)$ represent layer numbers of working windings A, superconducting winding B, and superconducting winding C, respectively.

The self-inductance and mutual inductance of three windings can be calculated as

$$L_A=\sum_{i=1}^{n_A}L_{A(i)A(i)}+\sum_{i=1}^{n_A}\sum_{\substack{j=1\\ i\neq j}}^{n_A}L_{A(i)A(j)} \tag{4}$$

$$L_B=\sum_{i=1}^{n_B}L_{B(i)B(i)}+\sum_{i=1}^{n_B}\sum_{\substack{j=1\\ i\neq j}}^{n_B}L_{B(i)B(j)} \tag{5}$$

$$L_C=\sum_{i=1}^{n_C}L_{C(i)C(i)}+\sum_{i=1}^{n_C}\sum_{\substack{j=1\\ i\neq j}}^{n_C}L_{C(i)C(j)} \tag{6}$$

$$M_{AB}=\sum_{i=1}^{n_A}\sum_{j=1}^{n_B}L_{A(i)B(j)} \tag{7}$$

$$M_{AC}=\sum_{i=1}^{n_A}\sum_{j=1}^{n_C}L_{A(i)C(j)} \tag{8}$$

$$M_{BC}=\sum_{i=1}^{n_B}\sum_{j=1}^{n_C}L_{B(i)C(j)} \tag{9}$$

Thus, the equivalent reactance of windings can be expressed as

$$X_A=jw(L_A-\frac{N_A}{N_B}M_{AB}-\frac{N_A}{N_C}M_{BC}+\frac{N_A^{\,2}}{N_BN_C}M_{AC}) \tag{10}$$

$$X_B=jw(\frac{N_A^{\,2}}{N_B^{\,2}}L_B-\frac{N_A}{N_B}M_{AB}-\frac{N_A^{\,2}}{N_BN_C}M_{AC}+\frac{N_A}{N_C}M_{BC}) \tag{11}$$

$$X_C=jw(\frac{N_A^{\,2}}{N_C^{\,2}}L_C-\frac{N_A}{N_C}M_{BC}-\frac{N_A^{\,2}}{N_BN_C}M_{AC}+\frac{N_A}{N_B}M_{AB}) \tag{12}$$

The magnetic flux circuit of SCR is shown in Fig.3. The magnetic path of capacity gear $G1$ is shown as $G1$, in which the main magnetic path mainly contains iron cores. The double-line represents the magnetic circuit of capacity gear $G2$, which consists of iron cores and air between superconducting winding C and working winding A. The magnetic circuit of capacity gear $G3$ includes iron cores and air between superconducting winding B and working winding A, which is shown by a short dash line. The magnetic circuit of $G1$ is represented by a solid line.

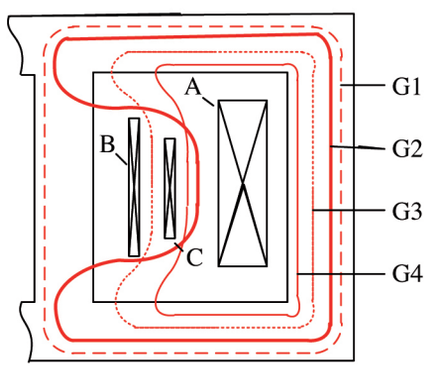

Fig. 3: Magnetic flux circuit of SCR

Hence, the reactance under different capacity gears can be expressed as

$$\begin{cases} X_{G1}=X_A+X_m \\ X_{G2}=X_A+X_B \\ X_{G3}=X_A+X_C \\ X_{G4}=X_A+X_B\,//\,X_C \end{cases} \tag{13}$$

The relationship between each reactance under different capacity gears is: $X_{G4}<X_{G3}<X_{G2}<X_{G1}$, whereas the relationship between different gear capacity is $S_{G1}<S_{G2}<S_{G3}<S_{G4}$.

3.2. TRANSIENT CHARACTERISTICS ANALYSIS OF SCR

The flux change of superconducting winding of a closed superconducting loop is shown in Fig.4. Ψ_0 is the flux through the superconducting winding. Ψ_a is the self-inductive flux produced by the current through the superconducting winding,

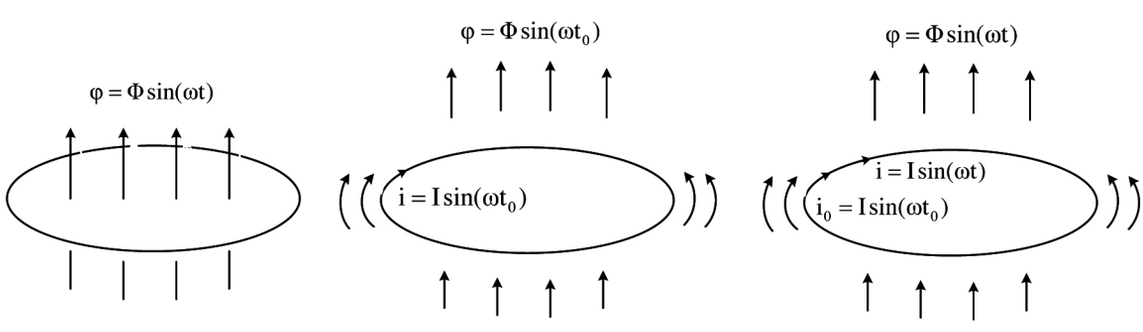

Fig. 4: Flux of a superconducting loop. (a) before closing the winding.(b) when closing the winding.(c) after closing the winding

$\psi_a = k\psi\sin(\omega\tau+\theta)$. k is the induction coefficient. i represents the current through the superconducting winding, and e is the induced electromotive force of the superconducting winding. The loop resistance $R=0$.

Based on Faraday's law of induction

$$\sum e = e_0 + e_a = -\frac{d(\Psi_a+\Psi_0)}{dt} = Ri = 0 \quad (14)$$

The total flux through the superconducting winding can be obtained

$$C=\Psi_a+\Psi_0 \quad (15)$$

If the superconducting loop is closed at $t=0$, then

$$\Psi_0 = k\Psi\sin(\theta) - k\Psi\sin(\omega t+\theta) \quad (16)$$

Hence, the DC flux is produced through the superconducting winding. This flux will induce the DC component in the superconducting winding.

When the superconducting winding of SCR is short-circuit, the resistance of superconducting winding $R=0$, the current of superconducting winding is

$$i = I_{pm}\sin(\omega t+\theta-\varphi)+C \quad (17)$$

where C is DC component, I_{m0} is the peak value of the periodic component, θ is the switching angle, and φ is the impedance angle.

Given that the current of superconducting winding cannot be changed at the switching time, the DC component can be expressed as

$$C = -I_{pm}\sin(\theta-\varphi) \quad (18)$$

The DC component will not decay and will make the cores become saturated, thereby producing more losses and harmonics. In addition, the DC component may lead to superconducting quench.

If the superconducting winding is cut off, then the current in inductance L_B will flow through the capacitor C_B (winding capacitor and winding-to-ground capacitor), as shown in Fig.5.

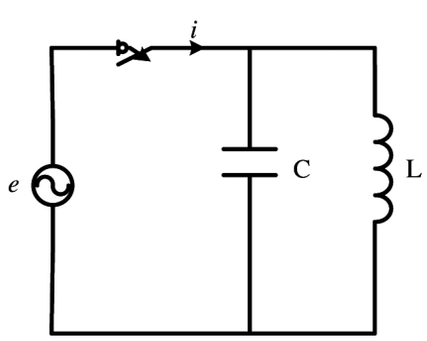

Fig. 5: The equivalent circuit on overvoltage of SCR

Given that the cut-off current of the winding is I_0 and the capacitor voltage is U_0, the energy of the superconducting winding can be expressed as

$$W = \frac{1}{2}L_B I_0^2 + \frac{1}{2}C_B U_0^2 \quad (19)$$

When all magnetic energies are transformed into electrostatic energies, the capacitor voltage will reach the maximum value U_{Bm}

$$\frac{1}{2}C_B U_{Bm}^2 = \frac{1}{2}L_B I_0^2 + \frac{1}{2}C_B U_0^2 \quad (20)$$

$$U_{Bm} = \sqrt{I_0^2\frac{L_B}{C_B}+U_0^2} \quad (21)$$

For superconducting winding. L_B is much larger than C_B. Hence, if the winding was not cut off at $I_0=0$, then the overvoltage would be huge and would easily cause the insulation damage of the superconducting winding.

3.3. OPTIMAL CONTROL STRATEGY OF SCR

To avoid producing DC component and overvoltage, the superconducting windings must be switched off/on when the currents of superconducting windings have reached zero. At this time, the flux through the superconducting windings has also reached zero.

$$\varphi = \Psi\sin(\omega t+\theta) = 0 \quad (22)$$

$$\omega t+\theta = k\pi \quad (23)$$

The voltage of working winding can be calculated as

$$e_1 = -N_1\frac{d\varphi}{dt} = -\omega N_1\Phi_m\cos(\omega t+\theta) \quad (24)$$

From (22) and (24), the phase difference between the flux of superconducting winding and the voltage of working winding is 90°. Hence, the superconducting windings should be switched off/on when the phase of voltage of working winding is $k\pi-90^0$.

In order to achieve the requirements above, an optimal transient control strategy based on circuit breaker and anti-parallel thyristors is proposed. Before switching on the superconducting winding, the anti-parallel thyristors are turned on at 90° of voltage phase of working winding for several cycles. Then, the superconducting winding is closed by a circuit breaker. In addition, before opening the superconducting winding, the anti-parallel thyristors are also turned on at 90° for several cycles until the circuit breaker is turned off completely, the current will be transferred to the anti-parallel thyristors. When the trigger pluses of the anti-

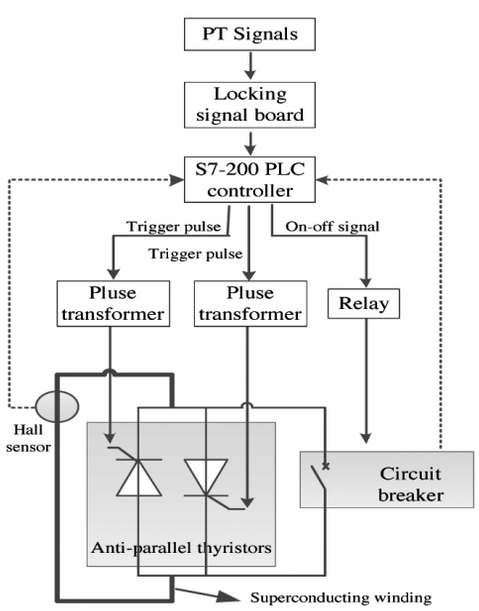

Fig. 6: Principle of control strategy of SCR

parallel thyristors are stopped, the thyristors will be turned off when the current is at zero point.

The principle of control strategy of SCR is shown in Fig.6. To ensure the reliability and stability of control system, Siemens S7-200 PLC is chosen as the controller. Firstly, the working voltage signals are acquired by the locking signal board to controller. When the capacity gear of SCR needs to be adjusted, a control signal is sent to a relay to control the circuit breaker, and pulse signals are sent to the pulse transformer to control the anti-parallel thyristors. The thyristor under a positive voltage will be turned on. In addition, when closing the superconducting windings, the anti-parallel thyristors can be turned on in the process of switching off the circuit breaker. The Hall current sensors are used to measure the currents of SCR.

4. RESULT ANALYSIS AND DISCUSSION

4.1. SIMULATION ANALYSIS OF SCR

In order to validate the principle and efficiency of methods proposed by this paper, a 380 V/30 kVar FEA model of SCR is designed. Various FEA simulation and optimization studies of SCR were performed in ANSYS. The capacity gears of SCR are: 0%, 80%, 90%, and 100%. Gear1 (G1: 0%) reflects no-load losses. The parameters of iron cores and windings are shown in Table II. The silicon steel sheet material of core is 30Q140, and its thickness is 0.30mm. The materials of superconducting windings are made up of Type H Sumitomo BISCCO.

Parameter	Value
Rated voltage/V	380
Rated capacity/kVar	30
Saturation flux density/T	1.65
Cross-sectional area of core/m2	0.0079
Height of cores /mm	455
Height of windings	410
Inner diameter of working winding	430
Turns of working winding	170
Inner diameter of superconducting winding B	156.44
Inner diameter of superconducting winding C	224.2
Turns of superconducting winding B and C	748

Table II : Parameters of SCR

The above parameters indicate that the impedance of SCR at different gears are calculated by simulation

$$X_{G1} = 207.65, X_{G2} = 6.09, X_{G3} = 5.22, X_{G4} = 4.95 \quad (25)$$

Based on the optimized method above, an optimal SCR FEA model with optimal parameters is designed. Various FEA simulations are performed to analyze the transient characteristics of SCR. The DC component of SCR is analyzed first. When the superconducting coil C is switched on at different angles of voltage phase of working winding A, the DC components are 100%, 70%, 50%, and 0%, when the superconducting winding is closed at 0°, 45°, 60°, and 90°, respectively. Hence, the results demonstrate that DC component of SCR is related to the angles of voltage phase of working winding A. To avoid the DC component, the superconducting winding should be switched on at 90°. The simulation waveforms at 0°, 45°, and 90° are shown in Fig.7.

Fig.8 shows the current and voltage of Superconducting windings when the capacity gear changes. When the superconducting winding C was switched on at 0.005s (90°), the capacity gear of SCR is changed from G1 to G2. Then at 0.025s (90°), the capacity gear of SCR is changed back to G1. This figure displays that almost no overvoltage occurs when superconducting winding is turned on and off at the voltage phase of 90°.

4.2. EXPERIMENTAL ANALYSIS OF SCR

In order to validate the principle and performance of SCR, a 380 V/30 kVar single-phase SCR laboratory prototype and control system were designed and tested, as shown in Fig.9 and Fig.10. The

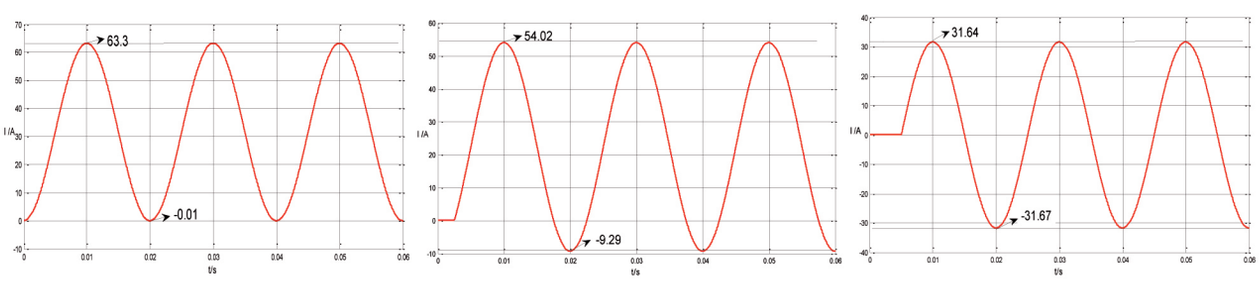

(a) *(b)* *(c)*

Fig. 7: DC component when superconducting winding is closed at different angles. (a) Superconducting winding is closed at 0°.(b) Superconducting winding is closed at 45°.(c) Superconducting winding is closed at 90°

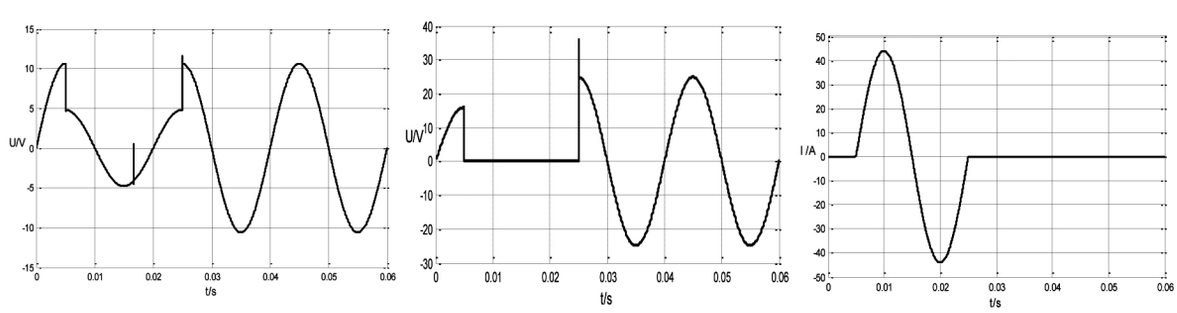

(a) *(b)* *(c)*

Fig. 8: Simulation results of overvoltage from G2 to G1. (a) Voltage of superconducting winding B.(b) Voltage of superconducting winding C.(c) Current of superconducting winding C

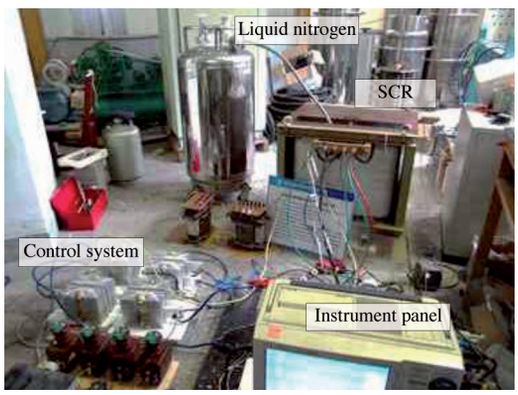

Fig. 9: Testing platform of 380V/30 kVA SCR

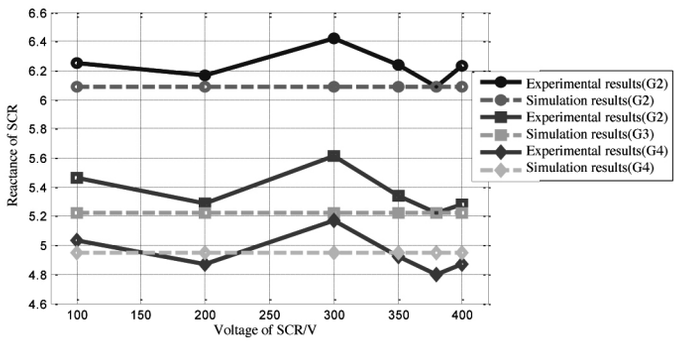

Fig.12: Comparison of impedance calculation results between simulation and experiment

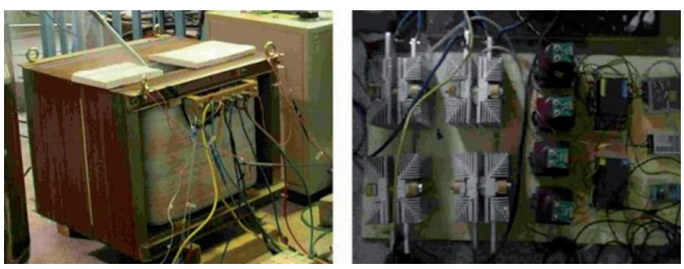

(a) *(b)*

Fig. 10: Prototype and control system of 380V/30 kVA SCR. (a) Prototype of SCR. (b) Control system of SCR

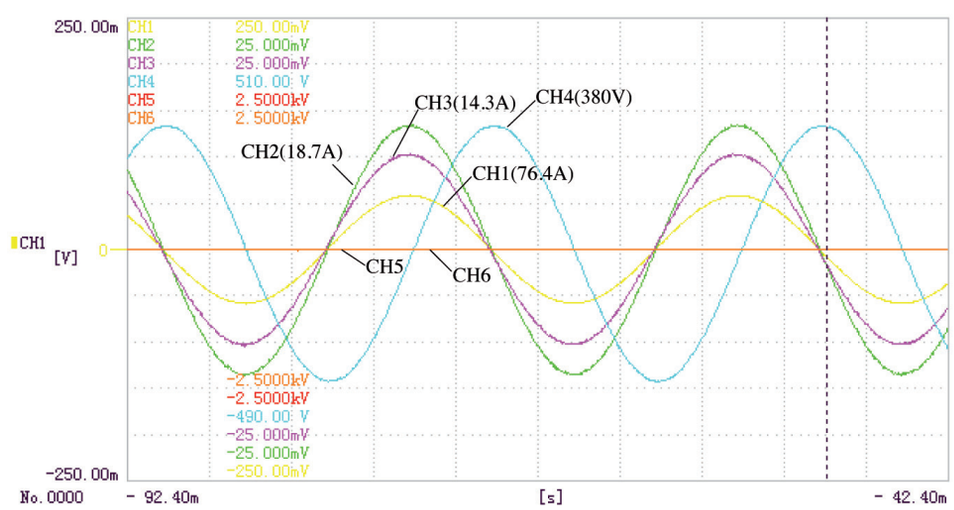

Fig. 11: Stead-state experimental results of SCR

design capacity gears of SCR prototype were 0%, 80%, 90%, and 100%. Superconducting windings were immersed in a Dewar filled with liquid nitrogen that maintained the temperature at 77 K. The control system was composed of anti-parallel thyristors, isolated pulse transformers, and Siemens S7-200 controllers. In addition, the experimental platform also included a 380V AC power supply and measuring instruments.

When the superconducting windings B and C were both closed, the capacity gear is G4, the stead-state experimental results of SCR are shown in Fig.11. CH1 represents current of working winding A, CH2 represents the current of superconducting winding B, and CH3 represents the current of superconducting winding C. Meanwhile, CH4 represents the voltage of working winding A and CH5 represents the voltage of superconducting winding B. In addition, CH6 represents the voltage of superconducting winding C. The steady-state results of SCR indicate that no harmonics and no overvoltage occurred. The SCR has a good performance on reactive power compensation.

The comparison of impedance calculation results between simulation and experiment is shown in Fig.12. The errors between experimental results and simulation results in G2, G3, and G4 are 2.2%, 2.8%, and 0.2%, respectively.

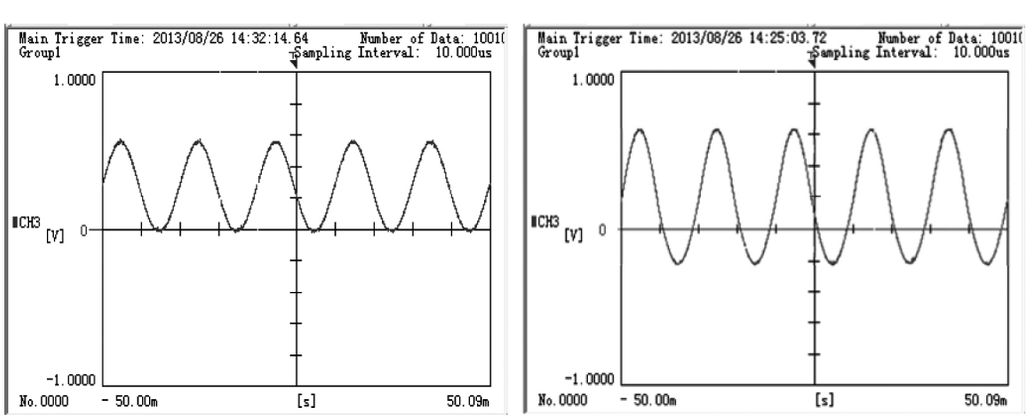

(a) *(b)*

Fig. 13: Experimental results when superconducting winding is closed at different angles. (a) Superconducting winding is closed at 0°.(b) Superconducting winding is closed at 60°

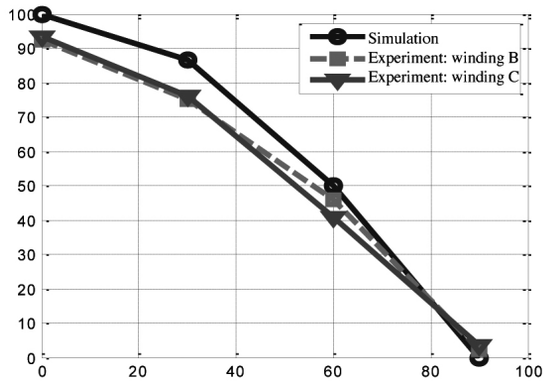

Fig. 14: DC component comparison between experiment and simulation

In order to validate the transient control characteristics and the optimal transient control strategy of SCR, the transient characteristics of SCR were tested. Fig.13 shows the current waveforms of working winding A when the superconducting winding C is closed at 0° and 60°. The DC component at the comparison of DC component of superconducting windings between experiment and simulation is shown in Fig.14.

The experimental results indicated that when the switching angle of superconducting winding changes from 0° to 90°, the DC component decreases gradually, similar to a sinusoidal wave. The largest DC component rate of superconducting windings B and C were 2.2% and 3.4% at 90°. The results between the experiment and simulation are almost identical. The small error of results is derived from the delay of the control system.

Fig.15 shows the overvoltage of superconducting windings when switching the capacity gears of SCR. The experimental results show that the overvoltage is excessively small with the optimal control system. The overvoltage times (maximum overvoltage/steady-state voltage peak) of superconducting windings in different gears are shown in Table III. The maximum overvoltage times is limited below 2.0 and has little effect on the insulation of superconducting windings. Hence, the experimental results demonstrate the effectiveness of optimal control system proposed in this paper.

4.3. DISCUSSION

When the superconducting winding is closing, the initial flux through the superconducting winding will induce the DC component. Since the resistance of superconducting winding is almost zero, the DC component will not decay. Moreover, when the switching angle of superconducting winding changes from 0° to 90°, the DC component will decrease gradually.

Additionally, when the superconducting winding is turning off, the magnetic energy of windings will be transferred to electrostatic field energy through the winding capacitor and winding-to-ground capacitor. Hence, the overvoltage of capacitor may be produced, when the winding is not cut off at I_0=0.

When the superconducting winding is controlled to switch off/on at voltage angle of 90°, the cut-off current and initial flux of superconducting winding is zero. There will be no overvoltage and DC component in the transient operation. Hence, the optimal control system is needed to avoid producing DC component and overvoltage of SCR.

According to the simulation and experimental results analysis, with the optimal control system proposed in this paper, the maximum DC component can be controlled below 3.4%, and the maximum overvoltage times is limited below 2.0 and has little effect on the insulation of superconducting windings. Therefore, it demonstrates that the optimal transient control strategy based on circuit breaker and anti-parallel thyristors can effectively reduce the DC component and overvoltage of superconducting windings. The small error of results is derived from the delay of the control system. The delay time would cause that the superconducting windings will not be switched on/off at 90°. Hence, in the design of control system, the delay time is needed to be considered. Moreover, the minor errors between the experimental and simulation results demonstrate the effectiveness of the simulation methods proposed in this paper.

Voltage	200V		350V		400V	
winding	B	C	B	C	B	C
G2 to G1	2.0	1.87	1.23	1.58	1.11	1.35
G3 to G1	1.37	1.37	1.29	1.35	1.84	1.84
G4 to G1	1.84	1.90	1.46	1.49	1.83	1.92

Table III:. Overvoltage times

5. CONCLUSION

In order to improve the performance of SCR, the transient characteristics analysis on DC component and overvoltage, and an optimal control strategy based on circuit breaker and anti-parallel thyristors were proposed. The mathematical impedance model of SCR is presented in detail, and the transient characteristics of SCR and the optimal control strategy are introduced. Via theoretical

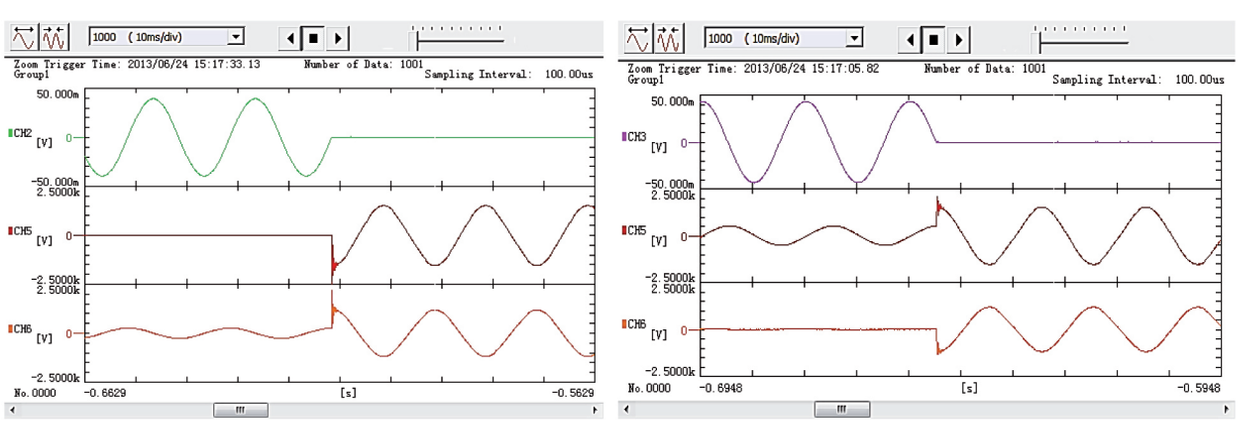

(a) *(b)*

Fig. 15: Experimental results of overvoltage. (a) From G2 to G1.(b) From G3 to G1

analysis, simulation, and experiments, the following conclusions were obtained:

(1) Based on the transient characteristics analysis of SCR, DC component and overvoltage would be produced in transient operation without optimal control strategy. The large DC component may drive the cores of SCR into saturation, resulting in producing more losses and harmonics, even leading to superconducting quench. In addition, the larger overvoltage will cause the insulation damage of the superconducting winding.

(2) To avoid DC component and overvoltage, the superconducting windings should be switched off/on when the voltage phase of working winding is 90°.

(3) The simulation and experimental results demonstrate that the optimal transient control strategy based on circuit breaker and anti-parallel thyristors can effectively reduce the DC component and overvoltage of superconducting windings.

In order to satisfy the operational requirements of the power system, the performance of SCRs, the control system in higher voltage class, and the influence on the stability of power system of SCR would be analyzed in future research.

BIBLIOGRAPHY

[1] Bai, J., Gu,W., Yuan, X., et al. "Power quality prediction, early warning, and control for points of common coupling with wind farms". Energies. August 2015. Vol. 8-9, p.9365–9382. DOI: http://dx.doi.org/10.3390/en8099365.

[2] Lei W, Lam C S, Man C W. "Design of A Thyristor Controlled LC Compensator for Dynamic Reactive Power Compensation in Smart Grid". IEEE Transactions on Smart Grid. 2016. p.1-1. DOI: http://dx.doi.org/10.1109/TSG.2016.2578178.

[3] Zhu G, Xiaowei D, Zhang C. "Optimisation of reactive power compensation of HVAC cable in off-shore wind power plant". IET Renew Power Generation. June 2015. Vol. 9-7, p.857-863. DOI: http://dx.doi.org/10.1049/iet-rpg.2014.0375.

[4] Boukadoum A, Bahi T. "Fuzzy logic controlled shunt active power filter for harmonic compensation and power quality improvement". Journal of Engineering Science & Technology Review. October 2014. Vol. 7-4, p.143-149.

[5] Bohmann L J, Lasseter R H. "Stability and harmonics in thyristor controlled reactors". IEEE Transactions on Power Delivery. April 1990. Vol. 5-2. pp.1175-1181. DOI: http://dx.doi.org/10.1109/61.53138.

[6] Haque S E, Malik N H. "Analysis and Performance of a Fixed Filter-Thyristor Controlled Reactor (FF-TCR) Compensator". IEEE Transactions on Power System. June1987. Vol. 2-2, p.303-309. DOI: http://dx.doi.org/10.1109/TPWRS.1987.4335123.

[7] Chen X, Chen B, Tian C. "Modeling and Harmonic Optimization of a Two-Stage Saturable Magnetically Controlled Reactor for an Arc Suppression Coil". IEEE Transactions on Industrial Electronics. July 2012. Vol. 59-7. p.2824-2831.DOI: http://dx.doi.org/10.1109/TIE.2011.2173090.

[8] Chen X, Chen J, Chen B. "Harmonic optimization for the multi-stage saturable magnetically controlled reactor using particle swarm optimization algorithm". In: proceedings of 2014 9th IEEE Conference on Industrial Electronics and Applications, Hangzhou, China, 9-11 June 2014. DOI: http://dx.doi.org/10.1109/ICIEA.2014.6931460.

[9] Young M, Dimitrovski A, Li Z, et al. "Gyrator-Capacitor Approach to Modeling a Continuously Variable Series Reactor". IEEE Transactions on Power Delivery. January 2015. Vol. 31-3. p.1-8. DOI: http://dx.doi.org/10.1109/TPWRD.2015.2510642.

[10] Rodríguez A, Bueno E J, Álvar Mayor. "Voltage support provided by STATCOM in unbalanced power systems". Energies. February 2014. Vol. 7-2. p.1003-1026. DOI: http://dx.doi.org/10.3390/en7021003.

[11] Chebabhi A, Fellah M K, Kessal A, et al. "Four Leg DSTATCOM based on Synchronous Reference Frame Theory with Enhanced Phase Locked Loop for Compensating a Four Wire Distribution Network under Unbalanced PCC Voltages and Loads". Journal of Power Technologies. 2016.

[12] Fujun M, An L, Qiaopo X, et al. "Derivation of zero-sequence circulating current and the compensation of delta-connected static var generators for unbalanced load". IET Power Electronics. March 2016. Vol. 9-3. p.576-588. DOI: http://dx.doi.org/10.1049/iet-pel.2014.0682.

[13] Isobe T, Shiojima D, Kato K, et al. "Full-bridge Reactive Power Compensator with Minimized Equipped Capacitor and its Application to Static Var Compensator". IEEE Transactions on Power Electronics. March 2015. Vol. 31-1. p.224-234. DOI: http://dx.doi.org/10.1109/TPEL.2015.2412954.

[14] Zhang Y, Lehner T F, Fukushima T, et al. "Progress in Production and Performance of Second Generation (2G) HTS Wire for Practical Applications". IEEE Transactions on Applied Superconducting. October 2014. Vol. 24-5, p.1-5. DOI: http://dx.doi.org/10.1109/TASC.2014.2340458.

[15] Dias D H N, Sotelo G G, Dias F J M, et al. "Characterization of a Second Generation HTS Coil for Electrical Power Devices". IEEE Transactions on Applied Superconducting. June 2015. Vol. 25-3, p.1-4. DOI: http://dx.doi.org/10.1109/TASC.2014.2366237.

[16] Shen S, Tang Y, Ren L, et al. "Development of a Leakage Flux-Controlled Reactor". IEEE Transactions on Applied Superconducting. June 2014. Vol. 24-3. p.1-5. DOI: http://dx.doi.org/10.1109/TASC.2013.2291156.

[17] Wamkeue R, Elkadri N E E, Kamwa I, et al. "Finite-Element Modelling of Multiple Rotor Circuits Synchronous Machines". International Journal of Simulation Modelling. July 2015. Vol. 22-4. p. 239-244.

[18] Bell S C, Bodger P S. "Inductive reactance component model for high-voltage partial-core resonant transformers". IET Electric Power Application, October 2008. Vol. 2-5. p.288-297. DOI: http://dx.doi.org/10.1049/iet-epa:20070452.

[19] Lapthorn A C, Chew I, Enright W G. "HTS Transformer: Construction Details, Test Results, and Noted Failure Mechanisms". IEEE Transactions on Power Delivery. February 2011.Vol. 26-1. p.394-399. DOI: http://dx.doi.org/10.1109/TPWRD.2010.2061874.